

Two Splice Variants of the Wilms' Tumor 1 Gene Have Distinct Functions during Sex Determination and Nephron Formation

Annette Hammes,¹ Jian-Kan Guo,¹
Gudrun Lutsch,¹ Joerg-Robert Leheste,¹
Danilo Landrock,¹ Ulrike Ziegler,¹
Marie-Claire Gubler,² and Andreas Schedl³

¹MDC for Molecular Medicine
Developmental Genetics
Robert-Rössle-Str. 10,
13092 Berlin
Germany

²Department of Pediatric Nephrology
Necker Hospital
75743 Paris cedex 15
France

Summary

Alternative splicing of *Wt1* results in the insertion or omission of the three amino acids KTS between zinc fingers 3 and 4. In vitro experiments suggest distinct molecular functions for + and –KTS isoforms. We have generated mouse strains in which specific isoforms have been removed. Heterozygous mice with a reduction of +KTS levels develop glomerulosclerosis and represent a model for Frasier syndrome. Homozygous mutants of both strains die after birth due to kidney defects. Strikingly, mice lacking +KTS isoforms show a complete XY sex reversal due to a dramatic reduction of *Sry* expression levels. Our data demonstrate distinct functions for the two splice variants and place the +KTS variants as important regulators for *Sry* in the sex determination pathway.

Introduction

The Wilms' tumor suppressor gene *Wt1* is a zinc finger gene mutated in a proportion of nephroblastomas, an embryonic kidney tumor found in 1 of 10,000 newborn. In vitro and in vivo studies suggest that *Wt1* can act as both a transcriptional repressor (Menke et al., 1998) and activator (Lee et al., 1999). A combination of alternative splicing, alternative translation start sites, and RNA editing leads to the expression of at least 24 different isoforms. Of particular interest are two alternative splice donor sites at the end of exon 9, leading to the insertion or omission of three amino acids (KTS) between zinc fingers 3 and 4 (designated as +KTS and –KTS isoforms). The alternative splice site is highly conserved during evolution and can be found in all vertebrates (Kent et al., 1995; Miles et al., 1998). Increasing evidence indicates that +KTS and –KTS isoforms serve distinct functions within the nucleus. –KTS isoforms are generally more active in transcriptional regulation, whereas +KTS products have been shown to colocalize with

splicing factors (Larsson et al., 1995; Ladomery et al., 1999; Englert et al., 1995). Biochemical studies show different properties of *Wt1* isoforms in their interaction with other proteins: e.g., the splicing factor U2AF65 has a stronger affinity to +KTS variants (Davies et al., 1998), whereas steroidogenic factor Sf1 binds preferentially to –KTS isoforms (Nachtigal et al., 1998). The two isoforms also differ in their binding affinity to nucleic acids. Indeed, in vitro studies (Caricasole et al., 1996) and computer modeling (Kennedy et al., 1996) suggest that +KTS proteins can bind to RNA, and it has been speculated that they may play a role in posttranscriptional modification. Finally, NMR relaxation experiments demonstrate that the insertion of the KTS sequence leads to an increased linker flexibility and loss of DNA binding of zinc finger 4, hence providing a molecular basis for the differential affinity of + and –KTS variants to DNA (Laity et al., 2000).

In addition to being a tumor suppressor gene, *Wt1* has been shown to fulfill important functions during embryonic development. Analysis of *Wt1* expression in the mouse demonstrated a developmentally dynamic expression pattern with an onset at E9.5 within the urogenital ridge (Armstrong et al., 1993). During kidney development, *Wt1* is expressed at low levels within the uninduced metanephric blastema, and increases during condensation and the formation of comma- and S-shaped bodies. In the adult kidney, *Wt1* remains to be expressed within the visceral epithelial cell layer of the mature glomerulus, the podocytes. During gonad development, *Wt1* expression can be found within the coelomic epithelial cell layer, as well as the developing Sertoli and granulosa cells of males and females, respectively. Interestingly, the expression of the different isoforms is tightly controlled, with a constant ratio for +KTS/–KTS variants in all tissues analyzed. Disturbance of this ratio is likely to result in severe abnormalities, at least in humans (see below).

Mice carrying homozygous knockout mutations of *Wt1* lack kidneys, gonads, and adrenal glands, and have defects in the formation of the heart (Kreidberg et al., 1993; Moore et al., 1999) and spleen (Herzer et al., 1999). The importance of *WT1* during development is also reflected by mutations, which lead to two developmental syndromes in man: the Denys-Drash syndrome (DDS) and Frasier syndrome (Gubler et al., 1999). DDS patients suffer from diffuse mesangial sclerosis, urogenital abnormalities, and a high risk of developing Wilms' tumor, whereas Frasier patients have focal segmental glomerular sclerosis, show male-to-female sex reversal, but do not usually develop tumors. Interestingly, *WT1* mutations in Frasier patients are found in intron 9, and affect the recognition of the second alternative splice donor site in the KTS region. As Frasier syndrome is caused by dominant mutations, it has been proposed that splice site mutation causes a shift of the ratio of +/-KTS isoforms toward the –KTS forms, rather than the complete deletion of +KTS variants (Barbaux et al., 1997; Klamt et al., 1998).

To generate a mouse model for Frasier syndrome,

³Present address and author for correspondence: School of Biochemistry and Genetics, University of Newcastle upon Tyne, Newcastle upon Tyne, United Kingdom, NE1 7RU, e-mail: andreas.schedl@ncl.ac.uk

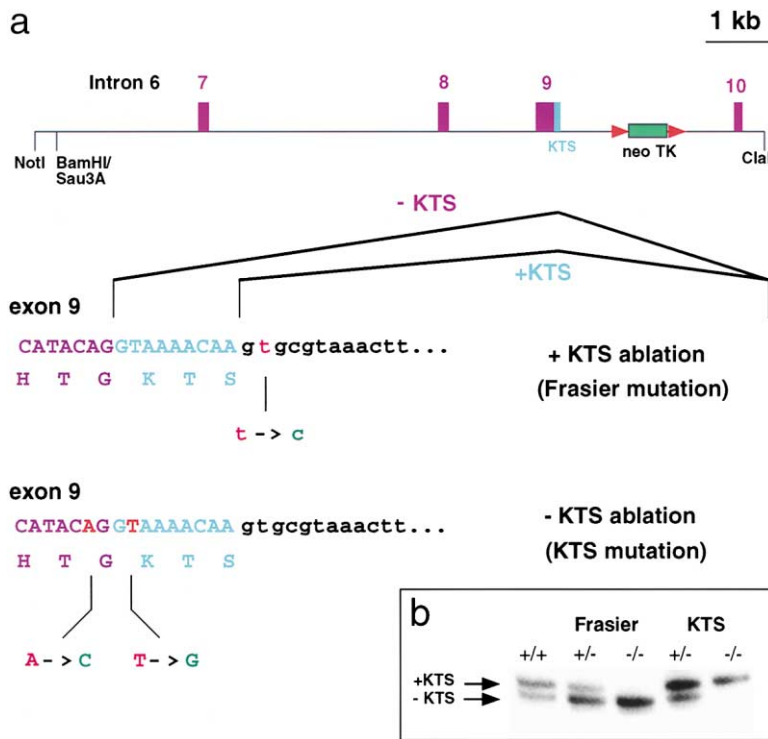


Figure 1. Gene Targeting at the Exon-Intron Boundary of *Wt1* Exon 9 Ablates Specific Isoforms In Vivo

(a) The targeting construct carrying the Frasier or KTS mutation was introduced into ES cells with a Neo-TK cassette flanked by lox sites located at intron 9 of *Wt1*. Subsequently, the cassette was removed by transient transfection with a CRE expressing plasmid. (b) RT-PCR analysis of RNA isolated from day 11.5 embryos. Primers homologous to exon 9 and 10 were used to amplify across the KTS region. Wild-type mice (+/+) show a ratio of 55/45 for + and -KTS, respectively. Mice heterozygous (+/-) for the Frasier and KTS mutation show the anticipated shift toward the -KTS and +KTS variants of *Wt1*, respectively. In mice homozygous (-/-) for the introduced mutations, only one band is visible, indicating complete ablation of the other forms.

and to clarify the function of the + and -KTS proteins in development, we have introduced specific mutations into the endogenous *Wt1* locus, designed to interfere with the production of one of the two variants. Here, we show that mice expressing only +KTS or only -KTS isoforms have severe defects in kidney and gonad formation. Importantly, +KTS and -KTS ablated mice show clearly different phenotypes, indicating distinct functions for the two splicing variants, in particular, in the sex determination pathway.

Results

Introduction of Point Mutations into the Splice Region of Exon 9 Specifically Ablates KTS Isoforms of *Wt1*

To ablate +KTS-specific isoforms, a mutation was introduced into the second splice donor site at position +2 in intron 9 (GT→GC) using a Cre-loxP strategy (Figure 1a). This mutation has been shown to result in Frasier syndrome in human patients (Kikuchi et al., 1998). -KTS ablation was achieved by replacing the 100% conserved GT of the first splice donor site in exon 9 with GG (the preceding codon was also changed from ACA to ACC to generate a restriction site for convenient identification of the mutation). The amino acid sequence (KTS) remained unchanged. For easier distinction of the two newly generated alleles, we will from now on refer to animals carrying the mutation for the +KTS ablation (Frasier mutation) as Frasier mice and for the -KTS ablation (KTS mutation) as KTS mice.

To exclude any negative effect caused by the presence of the loxP site in intron 9, we also employed a

double replacement strategy to introduce the Frasier mutation (GT → GC) into ES cells (details on request). One clone carrying the single nucleotide mutation was generated and used for the production of chimeric mice. Animals homozygous for this point mutation showed a phenotype identical to that found in mice generated with the Cre-loxP strategy. In addition, compound heterozygous mice carrying one KTS and one Frasier allele (generated by either the Cre-loxP or the double replacement strategy) developed normally. Hence, the detailed phenotypic analysis described below was performed using mice generated with the Cre-loxP strategy.

We next performed Northern blot analysis of RNA isolated from kidneys of newborn wild-type, heterozygous and homozygous mice to investigate the expression of *Wt1* RNA. No change of *Wt1* levels was detected, suggesting that the introduced mutations have no effect on the overall levels of *Wt1* RNA produced (data not shown). To investigate whether the introduced mutations had the desired effect on splicing, RNA isolated from day 10.5 and 11.5 embryos was subjected to quantitative RT-PCR analysis with primers in exon 9 and 10. Consistent with earlier publications, wild-type mice showed a ratio of 55/45 for +KTS/-KTS-specific splice isoforms (Figure 1b). In contrast, heterozygous Frasier and KTS mice showed the expected shift toward the -KTS and +KTS-specific isoforms, with ratios of 30/70 and 64/36, respectively. No additional bands were detected, indicating that no abnormal splice products were formed. Mice homozygous for the introduced mutations showed only one band (Figure 1b). Furthermore, primers designed to specifically detect +KTS isoforms did not yield any PCR product with RNA from mice homozygous for the Frasier mutation, whereas signals

were obtained with wild-type and $-KTS$ -ablated RNA (data not shown). Taken together, these data demonstrate that we have generated mice with a complete ablation of either $+KTS$ or $-KTS$ variants.

Splice-Specific Mutations Cause Defects in Kidney Development

Development of heterozygous KTS and Frasier mice was normal, and adults were fertile, producing normal numbers of offspring. After 2–3 months, however, a proportion of Frasier heterozygotes ($\sim 70\%$) developed severe albuminuria and died due to renal insufficiency. Histological analyses of affected kidneys demonstrated a combination of focal segmental glomerular sclerosis and diffuse mesangial sclerosis with dilatation of the tubular epithelium and protein casts (Figures 2a and 2b). Interestingly, Frasier mice crossed onto the C57/Bl6 strain (F1 generation) did not develop mesangial sclerosis within 6 months, suggesting that this phenotype is influenced by a strong genetic modifier(s).

We next analyzed the phenotype of mice homozygous for the splice mutations. In both genetic models, homozygous pups survived embryonic development, but then died within 24 hr after birth. Analysis of the urogenital system demonstrated severe kidney abnormalities, with characteristic red speckles due to localized macroscopic hemorrhage (Figures 2d and 2e). In contrast to wild-type and heterozygous littermates, the bladder was empty, indicating the absence of glomerular filtration.

Histological analysis of Frasier $-/-$ kidneys demonstrated an increase in stromal tissue and a decrease of tubular epithelium (Figure 2g). The blastema in the proliferating zone appeared slightly less condensed. The number of glomeruli was normal. Glomerular tufts, however, showed a reduction in size, with red blood cells leaking into the Bowman's space and proximal tubules (Figure 2j). Podocytes lacked the typical flattening along the glomerular basement membrane (GBM) and showed abnormal cytoplasmic vacuoles, and the formation of footprocesses was severely impaired (Figures 2j, 2n, and 2o). Immunohistochemical staining of sections with Wt1 and Pax2 antibodies was comparable to wild-type animals (Figures 3b and 3e). In contrast, synaptopodin (Figure 3h) and $\alpha 3$ -integrin (not shown) staining showed a much less complex glomerular structure, indicating defects in the formation of the glomerular tuft.

Homozygous KTS animals showed an even more severe phenotype. The dramatic reduction in kidney size (Figure 2e) was accompanied by an increase in the stromal component, a decrease in the nephrogenic zone (Figure 2h), and a reduction of the number of glomerular generations. Those glomeruli that did form were small and dramatically contracted (Figure 2k). Immunofluorescence analysis showed a normal distribution of Wt1 expression at all stages of nephron formation. Pax2, while normally distributed in wild-type and Frasier mice, showed a much looser appearance of the condensing blastema in KTS animals (Figure 3f). Strikingly, synaptopodin (Figure 3i) and $\alpha 3$ -integrin (data not shown) were almost entirely absent in homozygous KTS mice, with only the occasional glomeruli expressing low levels of these proteins. Taken together, these data demonstrate that the presence of both alternatively spliced isoforms

is crucial for normal kidney development, and particularly for the formation of a functional visceral epithelium.

KTS Isoforms Show Differential Nuclear Localization In Vivo

Results from in vitro studies have indicated different functions for $+$ and $-KTS$ isoforms. These distinct molecular properties have been reflected on the cellular level by a distinct nuclear localization of the isoforms. To investigate whether $+$ and $-KTS$ isoforms also show a distinct nuclear staining pattern in vivo, we performed immunohistochemical analysis on newborn kidneys. Wt1 staining in wild-type podocytes showed a predominantly diffuse staining, with some brighter speckles being visible (Figure 3j). A similar staining, but with slightly less obvious speckles, was visible in homozygous Frasier mice (Figure 3k). In contrast, Wt1 protein in KTS homozygous mice was clearly localized to speckles, supporting the hypothesis of distinct molecular roles for these splice variants (Figure 3l). 3D reconstructions of Wt1-stained nuclei confirmed these observations (available as supplemental data at <http://www.cell.com/cgi/content/full/106/3/319/DC1>).

A Splice-Specific Function During the Sex Determination Process

Analysis of gonads revealed distinct phenotypes in KTS and Frasier animals. Frasier homozygotes developed along the female pathway in both XY and XX animals. Histological analysis in XY Frasier mice showed the presence of germ cells, which, however, were fewer and not properly organized (Figure 4h). Ovaries of female Frasier mice developed normally. In contrast, gonads of homozygous KTS mice were dramatically reduced in size, lacked differentiated tissue (streak gonads in both male and female), and showed abnormal development of the genital ducts (Figure 4).

Wt1- KTS isoforms have been proposed to be transcriptional activators of the *Dax1* promoter (Kim et al., 1999). Since abnormally high levels of *Dax1* can interfere with male development (Swain et al., 1998), we analyzed the expression of this gene in our mouse models. At day E12.5, *Dax1* expression in wild-type males becomes restricted to the boundary of the mesonephros and genital ridge, whereas female mice show a more widespread expression throughout the gonad (Figures 5m and 5n). Strikingly, Frasier mice showed female-specific expression in both XY and XX embryos at day E12.5, confirming the sex reversal on the molecular level (Figures 5o and 5p). To explore whether increased expression of *Dax1* may be responsible for the observed phenotype, we performed quantitative RT-PCR on day 10.5 and 11.5 embryos. No significant increase compared to wild-type *Dax1* expression was observed in mice homozygous for the Frasier or KTS mutation at day 10.5 (Table 1). Similarly, real-time PCR analysis of *Lhx9*, *SF1*, and *GATA4*, three other genes involved in early gonadal development and differentiation, did not show overt differences between Frasier and wild-type animals (data not shown). In contrast, KTS animals at E11.5 expressed significantly lower values of *Dax1* compared to wild-type mice.

One of the earliest molecular markers of male develop-

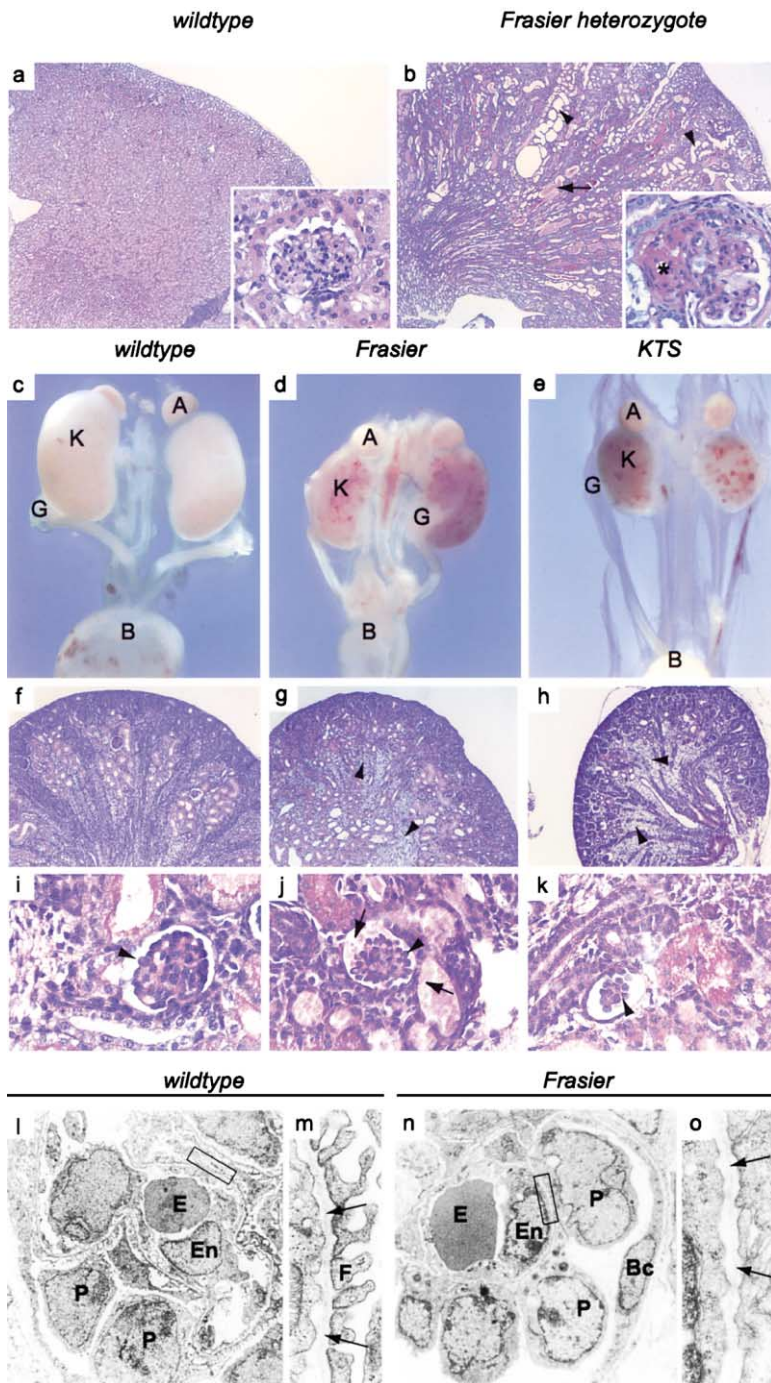


Figure 2. Kidney Phenotypes in Mice Heterozygous and Homozygous for Frasier and KTS Mutations

(a and b) PAS staining of adult kidneys in wild-type control and heterozygous Frasier mice (magnification: 10×; insets at 630×). Frasier heterozygotes develop severe mesangial sclerosis or focal segmental glomerular sclerosis (asterisk in inset), with dilatation of the proximal tubules (arrowhead) and protein casts (arrow). (c–e) Macroscopic view of the urogenital systems in wild-type and homozygous mutant mice at the day of birth. Frasier mice show a mild reduction of kidney size and develop local hemorrhage within the kidneys. In contrast, kidneys of KTS homozygotes are severely reduced. (A = adrenals, B = bladder, G = gonads, K = kidneys). (f–k) Histological analysis (PAS staining) of wild-type (f and i), Frasier (g and j), and KTS (h and k) kidneys at the day of birth (magnification, f–h = 100×; i–k = 630×). Frasier and KTS homozygotes show an increase in the stromal component of the kidney (arrowheads). Glomerular tufts in Frasier mice are generally less developed, with a lack of flattening of the podocytes (arrowheads). A proportion of glomeruli show leakage of erythrocytes (arrows) into the Bowman's space and the proximal tubule (j). KTS homozygotes show a reduction in the number of generations of glomeruli and severe glomerular contraction of those that formed (k). Electron microscopic analysis of Frasier animals (n and o) demonstrates impaired footprocess formation compared to wild-type littermates (l and m). Arrows indicate the glomerular basement membrane. Bc = Bowman's capsule, E = erythrocyte, En = endothelial cell, F = footprocess, P = podocyte. Magnifications: (l) and (n) = 3750×; (m) and (o) = 25000×.

ment is the transcription factor *Sox9*, which is expressed within the pre-Sertoli cells of the developing testis. Reduced expression of *SOX9* in man is sufficient to interfere with male development, and patients with mutations in this gene show male-to-female sex reversal, among other abnormalities (Wagner et al., 1994; Foster et al., 1994). In urogenital ridges of female mice, *Sox9* expression is restricted to the mesenchyme surrounding the Müllerian duct and the anterior boundary of the mesonephros and gonad. XY Frasier $-/-$ mice at embryonic day 11.5 and 12.5 showed the female-specific expres-

sion pattern for *Sox9* (Figure 5i, E12.5), suggesting that +KTS variants are required for the activation of this early marker gene. In contrast, expression of small amounts of *Sox9* could be detected in male KTS gonads in the region where male-specific *Sox9* expression is expected (Figure 5k). Similarly, expression of Müllerian inhibiting substance (*MIS*), which has been proposed to be a direct target of *Sox9* (Arango et al., 1999; De Santa Barbara et al., 1998), was also detectable in individual cells of the developing gonad in homozygous KTS animals (Figure 5s).

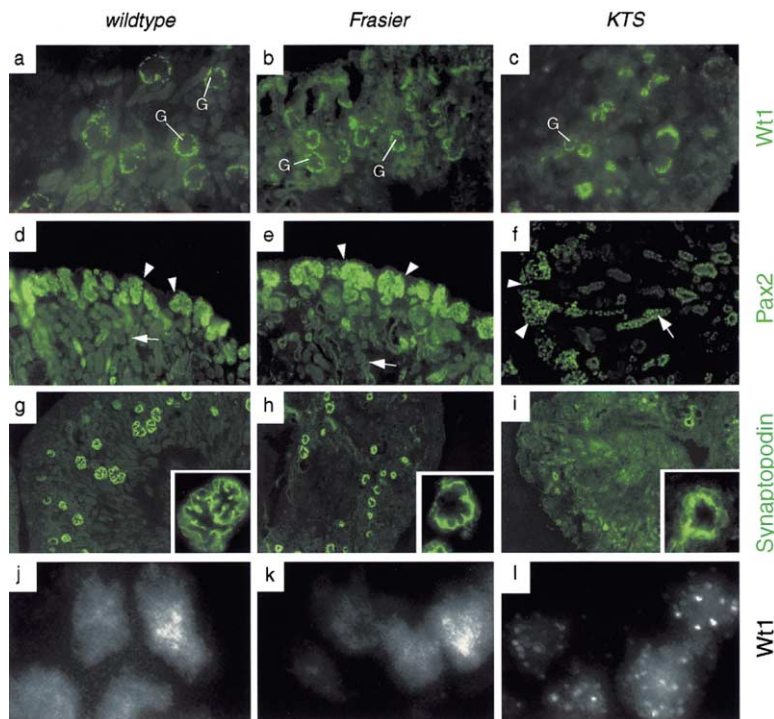


Figure 3. Immunohistochemical Analysis of Kidneys in Newborn Mice

The expression pattern for Wt1 (a–c) is normal in Frasier and KTS animals. (d–e) Pax2 staining in the condensing blastema (arrowheads) and collecting ducts (arrows) is also present in both models, but indicates less condensation of the mesenchyme in homozygous KTS animals (f). (g–i) Staining for synaptopodin shows the glomerular tuft to be less complex in Frasier (h) compared to wild-type (g) glomeruli. Synaptopodin expression in KTS homozygotes (i) is almost absent, with only the occasional glomerulus showing low levels of staining (magnification: 100 \times ; insets at 630 \times). (j–l) High-power view of WT1 staining in glomerular podocytes. Wild-type and Frasier mice show a more diffuse nuclear staining, whereas the Wt1 signal in KTS animals is almost entirely restricted to speckles. 3D reconstructions are available as supplemental data at <http://www.cell.com/cgi/content/full/106/3/319/DC1>.

Sex determination in mammals is initiated by the expression of the Y chromosome-encoded *Sry* gene. Given the absence of the early male-specific markers *Sox9* and *MIS*, we next investigated whether the Frasier mutation interfered with the expression of *Sry*. RNA was isolated from urogenital ridges of tail-somite-staged embryos (Hacker et al., 1995) and subjected to quantitative RT-PCR analysis. Wild-type animals showed the characteristic *Sry*-specific curve, with a peak of expression at E11.5 (tail somite stage \sim 18ts). Strikingly, *Sry* levels were significantly reduced in Frasier animals, to approximately 25% of that found in wild-type animals (Figure 6). We conclude that +KTS isoforms are essential for high levels of *Sry* expression, and hence, the initiation of the male sex determination pathway.

–KTS Isoforms Are Important for Cell Survival

The reduced size of gonads in KTS animals suggested either defects in proliferation or an increase in apoptosis. BrdU labeling at day 11.5 did not show obvious differences in the number of dividing cells between wild-type and KTS animals (data not shown). In contrast, TUNEL staining demonstrated an increased number of apoptotic cells in homozygous KTS mice in particular in the anterior region of the gonad (Figures 4m–4p). This increase of apoptosis is reflected in the lack of broadening of the genital ridge in both male and female KTS mice at day 11.5 (Figures 5e and 5f).

Discussion

KTS Splice Variants of Wt1 Have Redundant and Distinct Functions

The generation of Frasier and KTS animals allows us to draw conclusions about the *in vivo* function of the +

and –KTS isoforms in the mouse. Frasier mice have defects in the formation of the glomerular podocyte layer and the male sex determination process, but female gonads develop normally. In contrast, KTS animals have a much more pronounced phenotype, with hypodysplastic kidneys and the presence of streak gonads. Despite the severe phenotype in KTS gonads, several genes of the male sex determination cascade are expressed. Taken together, these results clearly demonstrate distinct roles for the two splice variants in development.

Despite these clear phenotypic differences, there are several organs affected in knockout mice, which seem to develop normally in our animals. For example, adrenal glands and spleen did not show overt abnormalities in either KTS or Frasier mice. Also, in kidney development, both isoforms can substitute for each other to some degree, and metanephric induction occurs in both models. The partial functional redundancy of +KTS and –KTS forms may seem surprising, considering their distinct nuclear localization. However, cell culture experiments indicate that removing the preferred target can change the nuclear distribution of Wt1 isoforms (Larsson et al., 1995). In addition, biochemical studies demonstrate that many targets of –KTS can also be bound by +KTS, albeit at a much reduced affinity.

We have observed no differences in the overall expression levels of *Wt1* mRNA in heterozygous or homozygous mice when compared to wild-type animals. This finding implies that the reduction of one of the alternatively spliced isoforms leads to an increase of the other. At the moment, we cannot exclude that such a mild overexpression of the unaffected isoform contributes to the observed phenotypes, and additional experiments using transgenic constructs should be done to clarify

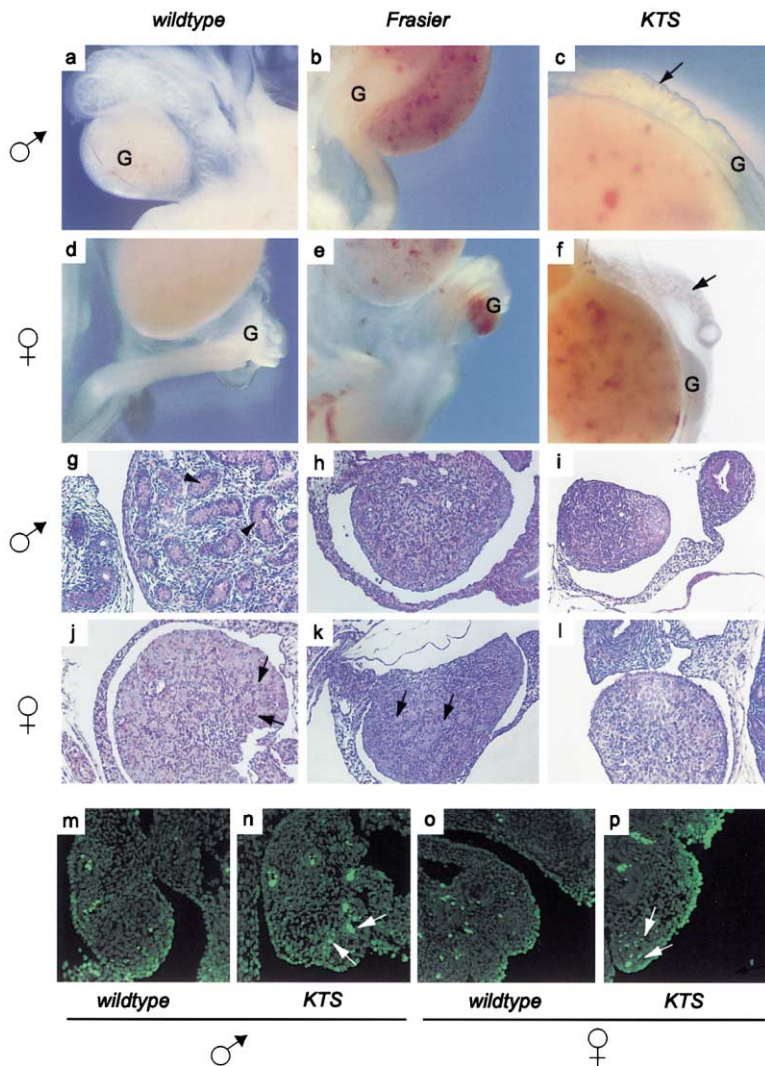


Figure 4. Phenotypic Analysis of Mutant Gonads

(a–f) macroscopic view of male and female gonads (G) at day 1 after birth. Both Frasier male (b) and female (e) gonads have an ovarian appearance and are not descended. In contrast, gonads in KTS animals are severely reduced in size (streak gonads) in both sexes, and show defects (c and f) in the differentiation of sexual ducts (arrows). (g–l) Light microscopic analysis of gonads (H&E staining). Frasier males (h) show the ground glass appearance of female gonads and a complete absence of seminiferous tubules (arrowhead in g). Gonads of female Frasier mice (k) are comparable to wild-type ovaries (j). Both male (i) and female (l) KTS animals show gonads of reduced size, with little signs of differentiation. (m–p) TUNEL assay of day 11.5 gonads. KTS homozygotes show reduced sizes and an increase in the number of apoptotic cells in the developing gonads (arrows).

this point. However, heterozygous KTS mice are normal despite an increase of +KTS variants, indicating, at least, that overexpression of +KTS isoforms does not cause developmental abnormalities.

It is surprising that Wt1 antibody staining in wild-type animals did not show a clearly discernible speckled pattern, which is in contrast to earlier studies (Larsson et al., 1995). These differences may be explained by the conventional fluorescent microscopy used for our analysis, in contrast to the confocal studies by Larsson et al. (1995). Alternatively, the lack of speckles may be due to interactions between +KTS and –KTS isoforms, which could result in +KTS forms being titrated away from speckles in wild-type animals. Our newly established mouse models will allow us to isolate cell lines, which specifically express +KTS or –KTS variants. These will be important tools to further explore the molecular function of the different isoforms.

A Mouse Model for Frasier Syndrome

Frasier patients display focal segmental glomerulosclerosis (FSGS) and a male-to-female sex reversal. We have

mimicked Frasier syndrome in the mouse by introducing a T-to-C mutation at position +2 of intron 9. Homozygous Frasier mice do not produce any +KTS isoforms, confirming the importance of the sequence downstream of exon 9 for proper splicing. Consequently, this region is highly conserved between mouse and man, and a comparison with the sequence of *Fugu rubripes WT1* shows only a single nucleotide exchange within 19 bp (Davies et al., 2000).

Also, on the phenotypic level, the Frasier mice strongly resemble the human syndrome, and heterozygous Frasier animals develop mesangial sclerosis from approximately 2 months onward. The kidney phenotype in our Frasier +/– mice is more pronounced than in human Frasier patients, with most of the glomeruli showing diffuse mesangial sclerosis rather than FSGS. Such a diffuse mesangial sclerosis is reminiscent of the kidney histology seen in Denys-Drash syndrome (DDS) patients, who have exonic mutations within the *WT1* gene. Hence, it is likely that the DDS phenotype in man is caused by a reduction of functional *WT1* due to dominant negative mutations. This hypothesis is strength-

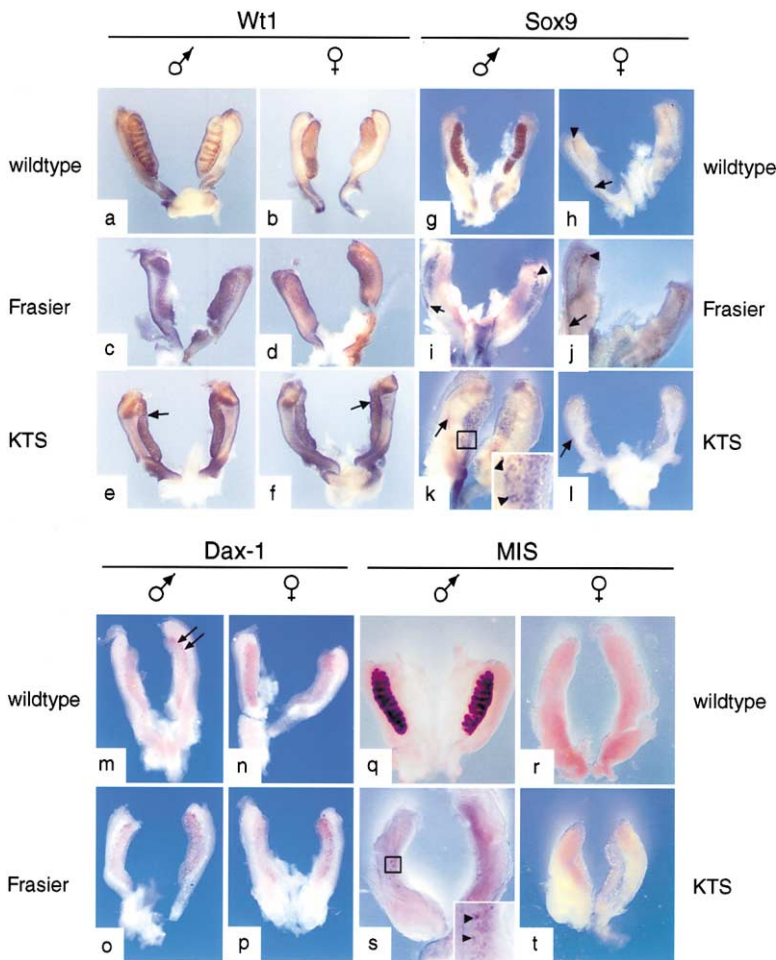


Figure 5. Whole Mount In Situ Hybridization of Sex Determining Genes

(a–f) Analysis of *Wt1* expression at day E12.5 shows the female-specific expression pattern in Frasier (c) and KTS (e) males. Note the reduction of gonad size in KTS homozygous animals (e and f arrow) compared to wild-type littermates and Frasier embryos. (g–l) At day E12.5, *Sox9* antisense probe shows the male-specific staining in wild-type gonads (g). Staining in females is restricted to the anterior end of the boundary between mesonephros and gonad (arrow) and the Müllerian duct mesenchyme (arrowhead). Staining in both male (i) and female (j) Frasier mice follows the female-specific pattern, indicating the importance of *Wt1* +KTS for the expression of *Sox9*. In contrast, KTS males show distinct cells expressing *Sox9* (arrowheads in k). (m–p) *Dax1* expression at E12.5 in male gonads is restricted to the boundary between mesonephros and gonad, but can be found throughout the gonad in female animals. Both XY and XX Frasier animals show the female-specific expression pattern. (q–t) *MIS* expression at E12.5 can be detected at high levels in wild-type males (q) but not in females (r). Consistent with results from the *Sox9* in situ hybridization (k), only very few cells express *MIS* in KTS males (s).

ened by recent results from other mouse models, which demonstrate that reduction of *Wt1* levels (our unpublished data) or the expression of a dominant negative mutant can cause mesangial sclerosis (Patek et al., 1999). Human patients suffering from isolated diffuse mesangial sclerosis (IDMS) should therefore be checked carefully for mutations within the splice region of exon 9. Indeed, *WT1* mutations have recently been identified in cases of IDMS (Ito et al., 1999). Heterozygous KTS mice did not develop any kidney disease, which suggests that the +KTS isoforms are more important for the maintenance of glomerular function.

Sex reversal as found in human patients never oc-

curred in heterozygous Frasier mice. This may suggest that the human sex determination pathway is generally more susceptible to small changes in gene expression. Alternatively, modifier gene(s) may influence the phenotype in man. The importance of +KTS variants in the sex determination pathway is, however, conserved between mouse and man, as homozygous Frasier mice show a complete sex reversal (see below).

The Role of *Wt1* in Kidney Development

Earlier studies have already demonstrated an important role of *Wt1* for several stages of kidney development (Kreidberg et al., 1993; Moore et al., 1999). Here, we

Table 1. Quantitative Analysis of *Dax1* Expression

| | Wild-type | | Frasier | | KTS | | <i>Wt1</i> Knockout | |
|-------|---------------|---------------|---------------|---------------|---------------|---------------|---------------------|---------------|
| | ♂ | ♀ | ♂ | ♀ | ♂ | ♀ | ♂ | ♀ |
| E10.5 | 3.04 n = 6 | 3.53 n = 5 | 3.01 n = 5 | 2.89 n = 5 | 3.35 n = 3 | 4.56 n = 3 | NA | 2.43 n = 3 |
| E11.5 | 5.04 n = 6 | 6.87 n = 9 | 7.1 n = 6 | 7.05 n = 3 | 1.31 n = 3 | 1.96 n = 4 | NA | NA |

RNA was isolated from embryos at day E10.5 to E11.5 and subjected to quantitative PCR using the LightCycler (mean values are given). No substantial differences in *Dax1* expression levels were detected at E10.5. However, at E11.5, homozygous KTS animals showed significantly lower levels.

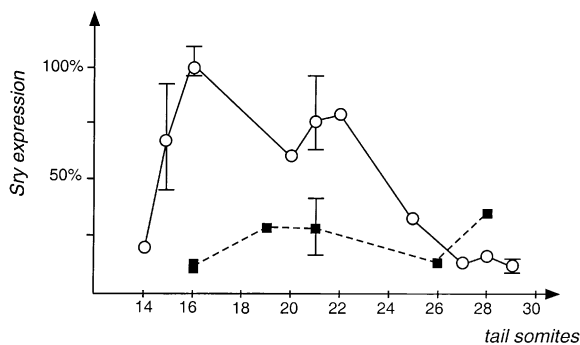


Figure 6. Quantitative SRY RNA Analysis in Wild-type and Frasier Animals

DNase treated RNA isolated from tail-somite staged embryos (E10.5–E12.5) was analyzed for the expression of *Sry*. Wild-type mice show a very dynamic expression pattern with a peak at approximately day E11.5 (16–18 ts). Frasier animals show a significant reduction of *Sry* levels to less than 25%, indicating the requirement of +KTS for *Sry* activation or stability.

have demonstrated that proper expression of + and –KTS isoforms of *Wt1* is important for the formation of a functional glomerulus. The early appearance of the phenotype and the complete absence of footprocesses suggest that *Wt1* +KTS is important for development of the podocyte architecture and the rigidity of the glomerular tuft.

The kidney phenotype in KTS $-/-$ mice was even more severe than in Frasier animals. The reduced size of the kidneys is likely to be due to increased apoptosis, as seen in mice expressing a hypomorph allele of *WT1* (Moore et al., 1999). The reduction of size in kidneys and gonads, as well as the increase in gonadal apoptosis in KTS animals, indicates that –KTS variants are very important for the survival of embryonic tissue. Interestingly, the number of convoluted proximal tubules per section was reduced in KTS animals, despite the fact that *Wt1* is not expressed in this epithelial tissue. Hence, we can speculate that factors derived from a functional glomerulus may stimulate the growth of the tubular epithelium. The almost complete absence of synaptopodin and $\alpha 3$ -integrin expression suggests that –KTS isoforms are required for an early differentiation step of the presumptive podocyte layer into the visceral epithelium.

The molecular mechanisms leading to the development of footprocesses are not very well understood. Recently, however, several genes involved in glomerular diseases have been cloned, most of which are structural proteins (Kestila et al., 1998; Kaplan et al., 2000; Boute et al., 2000; Shih et al., 1999). It is interesting to speculate that *Wt1* might regulate the expression or localization of one of these proteins. Certainly, the expression pattern of nephrin during kidney development is strikingly similar to that of *Wt1* (Putaalaa et al., 2000), and nephrin may represent a promising candidate for a downstream target of *Wt1*.

Wt1 Functions during the Sex Determination Process

The sex reversal found in Frasier patients and defects in gonad formation in DDS syndrome have implicated

Wt1 in gonad formation and sex determination. However, little is known about *Wt1* function during gonadogenesis at the molecular level. Kim et al. (1999) have shown that *Wt1* –KTS can activate the *Dax1* promoter, at least in vitro. The authors speculated that reduction of +KTS isoforms, as found in Frasier patients, could result in overexpression of –KTS variants and thus an overproduction of *Dax1*. Transgenic experiments suggest that increased levels of *Dax1* could indeed interfere with the male sex determination pathway (Swain et al., 1998). We could demonstrate that *Dax1* expression remains unchanged in Frasier animals, indicating a distinct mechanism for the observed sex reversal. Interestingly, mice lacking –KTS isoforms expressed decreased levels of *Dax1* at E11.5, which is in line with the proposed function of this variant as an activator of the *Dax1* promoter. Alternatively, the reduced levels of *Dax1* expression may be due to the increase of apoptosis in the gonads of homozygous KTS mice.

Shimamura et al. (1997), and more recently Hossain and Saunders (2001), have shown that *Sry* can be a target for *Wt1*, at least in vitro. In their experiments, *Sry* activation was only achieved using –KTS variants, whereas +KTS forms were completely inactive. In contrast, here we show that the *Wt1* +KTS variants are essential for high levels of *Sry* expression within the male gonad. A reduction of *Sry* expression to less than 30% of wild-type levels can indeed cause sex reversal in mice (Nagamine et al., 1999). At the moment, we cannot distinguish between a requirement of +KTS isoforms for transcriptional activation and for the stability of *Sry* by binding to its RNA. Clearly, the reduced level of *Sry* leads to the absence of *Sox9* expression in the developing XY gonad and, consequently, development along the female pathway. Homozygous KTS animals express *Sox9* and *MIS*, at least in a subset of cells, implying that the sex determination pathway in this strain is not completely blocked.

In conclusion, our data suggest two distinct functions for *Wt1* in gonad formation and sex determination. Proliferation of the coelomic epithelium leads to the development of the undifferentiated gonad. –KTS isoforms are required for the survival of the gonadal primordium, and KTS mice show increased apoptosis. In male gonads, the sex determination process is initiated by the expression of *Sry*. Absence of +KTS variants leads to a reduction of *Sry* expression levels and, consequently, the absence of *Sox9* and *MIS* activation.

Experimental Procedures

Construction of Targeting Vectors

Description of experimental details will be restricted to the Cre-lox based strategy. Details on the double replacement strategy used are available on request. An 8 kb fragment, including parts of intron 6 down to the first 50 bp of exon 10, was isolated from a 129 mouse BAC (Genome systems) by partial digestion, cloned into pBluescript II SK (+) and used for construction of the targeting vector. Point mutations were introduced using PCR-based mutagenesis. Primers for the +KTS ablation: forward primer, 5' GTT TTC CCG GTC CGA CCA TCT GAA GAC CCA CAC CAG GAC TCA TAC AGG TAA AAC AAG CGC GTA AAC 3'; T7 reverse primer, 5' GTA ATA CGA CTC ACT ATA GGG C 3' (point mutation underlined). The point mutation created a new *CfoI* site (bold). Primers for the –KTS ablation: forward primer, GTT TTC CCG GTC CGA CCA TCT GAA GAC CCA

CAC CAG GAC TCA TAC CGG GAA AAC AAG (point mutations underlined). The first point mutation created an additional HpaII site; the second point mutation was set to destroy the first splice donor site for the KTS region. The mutations were introduced into the targeting vector by replacing a 2.4 kb RsrII-ClaI fragment with a long-range PCR product (Roche) obtained with the above primers. Finally, a 3.6 kb HSVtk-PGK-Neo-Poly(A) selection cassette flanked by loxP sites from the vector pFlox (kindly provided by T. Willnow, MDC Berlin) was placed into a unique Ball site 1 kb downstream of exon 9.

Transfection and Selection of ES Cells

AB1 ES cells were grown on embryonic fibroblast feeder (Willnow and Herz, 1994), electroporated with 80 μ g of NotI linearized targeting vector, and after 12 hr, neomycin selection was applied at a final active concentration of 190 ng/ μ l G418 (Gibco BRL). Positive ES clones were expanded, electroporated in the presence of 50 μ g circular pMC-Cre plasmid (courtesy of K. Rajewsky), and plated in dilutions of 1:100 to 1: 5000. After 3 days, selection for the loss of the neo-TK cassette was performed using Gancyclovir at a final concentration of 2 μ M. Positive ES cell clones (see below) were injected into C57/Bl6 blastocyst as described by Bradley (1987).

Analysis of Genomic ES Cell DNA

Homologous recombination in the first targeting event was confirmed by Southern blot analysis (BamHI and SpeI digest) and PCR (details on request). Screening for the point mutation after the second selection of ES cells was performed using 10 pg to 1 ng of genomic DNA using the following PCR conditions: denaturation at 95°C for 10 min; 32 cycles at 95°C for 45 s, at 60°C for 45 s, and at 72°C for 45 s; final extension at 72°C for 10 min. (Exon 9 forward primer: 5'-GTG AAA CCA TTC CAG TGT AAA AC-3'; Intron 9 reverse primer 5'-GCT CAT TGA CCC TTT CTC TG-3'). Subsequently, the 276 bp PCR product was digested with CfoI (KTS) and HpaII (Frasier) and separated on a 3% agarose gel.

Primers for Determining the Sex of Animals

The presence of the Y chromosome was determined using primers for the Zfy and Sry genes as described by Hogan et al. (1994).

Expression Analysis

Embryonic tissue was dissected from staged embryos in PBS on ice and snap frozen in liquid nitrogen. DNA-free RNA was prepared using Absolutely RNA RT-PCR kit (Stratagene) or RNeasy (Qiagen). Detection of linear Sry transcripts was performed as described by Toyooka et al. (1998).

Detection of +/-KTS Variants by RT-PCR

Wt1 exon 9 forward primer (5'-GTGAAACCATTCAGTGTA AAC) was end labeled with γ -³²P-ATP and combined with exon 10 reverse primer (5'-GCCACCGACAGCTGAAGGGC); PCR conditions: denaturation at 95°C for 10 min; 28 cycles at 95°C for 45 s, at 60°C for 45 s, and at 72°C for 45 s; final extension at 72°C for 5 min. 10 μ l of PCR products were separated on a 12% PAGE-gel (fragment sizes: +KTS, 117 bp; -KTS, 108 bp). Signals were quantified using a Fuji BAS 2000 Imager.

The absence of +KTS isoforms in the Frasier mice was confirmed by PCR using exon 9 forward primer: 5'-GTGAAACCATTCAGTG TAA AAC 3' and exon 9-10 reverse primer: 5'-GGG CTTTCACTTGT TTTAC 3' (PCR conditions as above, but 35 cycles, expected fragment of 101 bp).

Quantitative RT-PCR Analysis

RNA for *Dax1* expression analysis was extracted from day 10.5 and 11.5 embryos and subjected to two-step RT-PCR. *Dax1* levels were quantified with a LightCycler kit (DNA Master Hybridization Probes; Roche) using primers 5'-AGATGATGGAGATCCCGAG and 5'-TCA CAGCTTGCACAGAGCA for amplification and LC-Red640-CCTG GTGGTAAGCATTTCTGCGTC-p and GCTCTGGACCTTCGGTCTC CTGCC-X as hybridization probes. Series dilutions of *Dax1* cDNA were used to generate the standard curve.

For the analysis of *Lhx9*, *GATA4*, *SF1*, and *Sry* expression levels, urogenital ridges of embryos staged by tail somite counting

were microdissected, RNA-extracted and subjected to quantitative RT-PCR using the following primers: *Lhx9*: Primers, 5'-TATCC ACCTCAGCTGAGCTACAC and 5'-CAAGTGGTCTGCCTCGTCTCT; hybridization probes, 5'-TTCTGCACGGTGCCAGTGCCATT-X and LC-Red640-AAGTAAGGCAAAGCCAAGCCGCC-p; *GATA4*: Primers, 5'-TCCCCACAAGGCTATGCATCT and 5'-CCCAGAACACCCATAT CCTAAG; hybridization probes, 5'-GCTGATTACGGCGGTGATTAT GTCCC-X and LC-Red640-ATGACTGTCAGCCAGGACCAGGC-p; *SF1*: Primers, 5'-TTCTGAGAGCCCGCTAGCC and 5'-CCTCGTC GTACGAGTAGTCCATG; hybridization probes, 5'-CCTGGTGTCC AGTGTCCACCCT-X and LC-Red640-TCCGGCTGAGAATTCCTCC TTCCG-p; *Sry*: Primers, 5'-AAGCTGTGTTTCAAGGGCTAG and 5'-TTGAGGGGTTGCTGTGTAC; hybridization probes, 5'-CAATC TGGCAGTTGAGTTAATGTGCAGAT-X and LC-Red640-CCATTCAT TCATCCCACATATACTTGCCC-p. The individual samples were standardized by measuring the amount of GAPDH RNA using quantitative PCR (primers, 5'-ATTCAACGGCACAGTCAAGG and 5'-TGGAT GCAGGGATGATGTTTC; hybridization probes, 5'-CCAGAAGACTGT GGATGGCCCCT-X and LC-Red640-TGGAAAGCTGTGGCGTGAT GGC-p).

Histological Analysis

Newborn mice were sacrificed by decapitation. The urogenital tracts were dissected, fixed with 4% paraformaldehyde in 1 \times PBS at 4°C overnight, and embedded in paraffin. Sections were cut at 1–2 μ m thickness and stained with PAS (periodic acid and Schiff staining plus hematoxylin counterstain) or H&E (hematoxylin, eosin).

Immunohistochemistry

Kidneys from newborn mice were rinsed in PBS, fixed with 4% paraformaldehyde in PBS (30 min, 4°C), rinsed again twice in PBS, and incubated in 20% sucrose at 4°C. The following day, tissues were embedded in O.C.T. (TissueTek) and frozen on dry ice. Cryosections were cut at 8–10 μ m and placed on TESPA coated slides. Immunostaining was carried out as described by Moore et al. (1999), using antibodies from Santa Cruz Biotechnology (WT1: C-19, cat# sc-192; Integrin α 3: c-18, cat# sc-6587) and BabCO Inc. (Pax2: cat# PRP-276P). The polyclonal antibody against synaptopodin was kindly provided by Peter Mundel (New York). Fluorescent conjugated secondary antibodies were purchased from Jackson ImmunoResearch Laboratories, Inc. The following dilutions were used: *Wt1*, 1:20; Pax 2, 1:100; Integrin α 3, 1:100; Synaptopodin, 1:50; 2nd antibody, 1:100. Stained sections were examined and photographed with a Zeiss Axioplan2 imaging microscope with a SPOT-RT camera and Metamorph (V.4.1.2) software.

Electron Microscopy

Cortical tissue of kidneys of newborn mice was fixed in a solution containing 4% formaldehyde, 2.5% glutaraldehyde, 2 mM CaCl₂, and 0.1 M cacodylate buffer, pH 7.2, for 2 h at room temperature. Postfixation was carried out with 2% osmium tetroxide and 4% uranyl acetate for 1 h at room temperature in both cases. Tissue pieces were dehydrated in a graded series of ethanol and embedded in PolyBed 812 (Polysciences, UK). Ultrathin sections of 70 nm thickness were prepared with an ultracut S ultramicrotome (Leica, Bensheim, Germany) and stained with lead citrate. Electron micrographs were taken with an EM 910 electron microscope (LEO, Oberkochen, Germany).

Whole Mount In Situ Hybridization

Urogenital ridges from 12.5 dpc embryos were dissected free from other internal organs and left attached to the back. Tissues were fixed with 4% PFA in PBS over night at 4°C. Further processing of embryos and in situ hybridization was carried out essentially as described by Wilkinson (1992). *Sox9* probes were synthesized according to Morais da Silva et al. (1996). The *MIS* plasmid was kindly provided by Holly Ingraham (San Francisco). The mouse *Wt1* riboprobe was generated from a cDNA subcloned into pBluescript (details on request). The vector to synthesize the *Dax1* probe was generated by cloning a RT-PCR product into pBluescript II SK (+). (forward primer: 5'-TCAGGAAGAGCGAGAG and reverse primer: 5'-ACACCACCTGTGGATCC (Swain et al., 1996). Antisense and sense

digoxigenin-labeled riboprobes were synthesized by in vitro transcription using T7- or T3-polymerase (USB).

Apoptosis Analysis

Urogenital ridges from 11.5 dpc embryos were dissected, fixed, embedded, and sectioned as described above. After dewaxing and rehydration the sections were incubated with 20 µg/ml proteinase K in 10 mM Tris/HCl pH 7.4 for 20 min at 37°C. Detection of apoptotic cells was performed using the TUNEL reaction kit (Roche) following manufacturer's instructions.

Acknowledgments

We would like to thank Irene Thun for histological sectioning, Erika Kotischke for assistance in electron microscopy, Olfert Landt from TIB Molbiol for LightCycler probe design, Ulrike Stein for advice on real-time PCR, and Peter Mundel for the generous gift of the synaptopodin antibody. We are grateful to Marie-Christine Chaboisier for helpful discussions, and Valerie Vidal, Frances Wong, and Gary Lewin for critically reading the manuscript. This work was supported by a grant from the DFG (SCHE564/1-1) and the European Community (QLRT00742).

Received November 15, 2000; revised July 3, 2001.

References

Arango, N.A., Lovell-Badge, R., and Behringer, R.R. (1999). Targeted mutagenesis of the endogenous mouse *Mis* gene promoter: in vivo definition of genetic pathways of vertebrate sexual development. *Cell* 99, 409–419.

Armstrong, J.F., Pritchard Jones, K., Bickmore, W.A., Hastie, N.D., and Bard, J.B. (1993). The expression of the Wilms' tumour gene, *WT1*, in the developing mammalian embryo. *Mech. Dev.* 40, 85–97.

Barboux, S., Niaudet, P., Gubler, M.C., Grunfeld, J.P., Jaubert, F., Kuttann, F., Fekete, C.N., Souleyreau Therville, N., Thibaud, E., Fellous, M., and McElreavey, K. (1997). Donor splice-site mutations in *WT1* are responsible for Frasier syndrome. *Nat. Genet.* 17, 467–470.

Boute, N., Gribouval, O., Roselli, S., Benessy, F., Lee, H., Fuchshuber, A., Dahan, K., Gubler, M.C., Niaudet, P., and Antignac, C. (2000). *NPHS2*, encoding the glomerular protein podocin, is mutated in autosomal recessive steroid-resistant nephrotic syndrome. *Nat. Genet.* 24, 349–354.

Bradley, A. (1987). Production and analysis of chimeric mice. In *Teratocarcinomas and Embryonic Stem Cells: A Practical Approach*, E.J. Robertson, ed. (Oxford: IRL Press), pp. 113–151.

Caricasole, A., Duarte, A., Larsson, S.H., Hastie, N.D., Little, M., Holmes, G., Todorov, I., and Ward, A. (1996). RNA binding by the Wilms tumor suppressor zinc finger proteins. *Proc. Natl. Acad. Sci. USA* 93, 7562–7566.

Davies, R.C., Calvio, C., Bratt, E., Larsson, S.H., Lamond, A.I., and Hastie, N.D. (1998). *WT1* interacts with the splicing factor U2AF65 in an isoform- dependent manner and can be incorporated into spliceosomes. *Genes Dev.* 12, 3217–3225.

Davies, R.C., Bratt, E., and Hastie, N.D. (2000). Did nucleotides or amino acids drive evolutionary conservation of the *WT1* +/-KTS alternative splice? *Hum. Mol. Genet.* 9, 1177–1183.

De Santa Barbara, P., Bonneaud, N., Boizet, B., Desclozeaux, M., Moniot, B., Sudbeck, P., Scherer, G., Poulat, F., and Berta, P. (1998). Direct interaction of *SRY*-related protein *SOX9* and steroidogenic factor 1 regulates transcription of the human anti-Mullerian hormone gene. *Mol. Cell. Biol.* 18, 6653–6665.

Englert, C., Vidal, M., Maheswaran, S., Ge, Y., Ezzell, R.M., Isselbacher, K.J., and Haber, D.A. (1995). Truncated *WT1* mutants alter the subnuclear localization of the wild-type protein. *Proc. Natl. Acad. Sci. USA* 92, 11960–11964.

Foster, J.W., Dominguez Steglich, M.A., Guioli, S., Kowk, G., Weller, P.A., Stevanovic, M., Weissenbach, J., Mansour, S., Young, I.D., Goodfellow, P.N. (1994). Campomelic dysplasia and autosomal sex reversal caused by mutations in an *SRY*-related gene. *Nature* 372, 525–530.

Gubler, M.C., Yang, Y., Jeanpierre, C., Barboux, S., and Niaudet, P. (1999). *WT1*, renal development, and glomerulopathies. *Adv. Nephrol. Necker Hosp.* 29, 299–315.

Hacker, A., Capel, B., Goodfellow, P., and Lovell Badge, R. (1995). Expression of *Sry*, the mouse sex determining gene. *Development* 121, 1603–1614.

Herzer, U., Crocoll, A., Barton, D., Howells, N., and Englert, C. (1999). The Wilms tumor suppressor gene *wt1* is required for development of the spleen. *Curr. Biol.* 9, 837–840.

Hogan, B.L., Beddington, R.S., Constantini, F., and Lacy, E. (1994). *Manipulating the Mouse Embryo*. (Cold Spring Harbor: Cold Spring Harbor Laboratory Press).

Hossain, A., and Saunders, G.F. (2001). The human sex-determining gene *sry* is a direct target of *wt1*. *J. Biol. Chem.* 276, 16817–16823.

Ito, S., Ikeda, M., Takata, A., Kikuchi, H., Hata, J., and Honda, M. (1999). Nephrotic syndrome and end-stage renal disease with *WT1* mutation detected at 3 years. *Pediatr. Nephrol.* 13, 790–791.

Kaplan, J.M., Kim, S.H., North, K.N., Rennke, H., Correia, L.A., Tong, H.Q., Mathis, B.J., Rodriguez-Perez, J.C., Allen, P.G., Beggs, A.H., and Pollak, M.R. (2000). Mutations in *ACTN4*, encoding alpha-actinin-4, cause familial focal segmental glomerulosclerosis. *Nat. Genet.* 24, 251–256.

Kennedy, D., Ramsdale, T., Mattick, J., and Little, M. (1996). An RNA recognition motif in Wilms' tumour protein (*WT1*) revealed by structural modelling. *Nat. Genet.* 12, 329–331.

Kent, J., Coriat, A.M., Sharpe, P.T., Hastie, N.D., and van Heyningen, V. (1995). The evolution of *WT1* sequence and expression pattern in the vertebrates. *Oncogene* 11, 1781–1792.

Kestila, M., Lenkkeri, U., Mannikko, M., Lamerdin, J., McCready, P., Putaala, H., Ruotsalainen, V., Morita, T., Nissinen, M., Herva, R. (1998). Positionally cloned gene for a novel glomerular protein—nephrin—is mutated in congenital nephrotic syndrome. *Mol. Cell* 1, 575–582.

Kikuchi, H., Takata, A., Akasaka, Y., Fukuzawa, R., Yoneyama, H., Kurosawa, Y., Honda, M., Kamiyama, Y., and Hata, J. (1998). Do intronic mutations affecting splicing of *WT1* exon 9 cause Frasier syndrome? *J. Med. Genet.* 35, 45–48.

Kim, J., Prawitt, D., Bardeesy, N., Torban, E., Vicaner, C., Goodyer, P., Zabel, B., and Pelletier, J. (1999). The Wilms' tumor suppressor gene (*wt1*) product regulates *Dax-1* gene expression during gonadal differentiation. *Mol. Cell. Biol.* 19, 2289–2299.

Klamt, B., Koziell, A., Poulat, F., Wieacker, P., Scambler, P., Berta, P., and Gessler, M. (1998). Frasier syndrome is caused by defective alternative splicing of *WT1* leading to an altered ratio of *WT1* +/-KTS splice isoforms. *Hum. Mol. Genet.* 7, 709–714.

Kreidberg, J.A., Sariola, H., Loring, J.M., Maeda, M., Pelletier, J., Housman, D., and Jaenisch, R. (1993). *WT-1* is required for early kidney development. *Cell* 74, 679–691.

Ladomery, M.R., Slight, J., Mc, G.S., and Hastie, N.D. (1999). Presence of *WT1*, the Wilms' tumor suppressor gene product, in nuclear poly(A)(+) ribonucleoprotein. *J. Biol. Chem.* 274, 36520–36526.

Laity, J.H., Dyson, H.J., and Wright, P.E. (2000). Molecular basis for modulation of biological function by alternate splicing of the Wilms' tumor suppressor protein. *Proc. Natl. Acad. Sci. USA* 97, 11932–11935.

Larsson, S.H., Charlier, J.P., Miyagawa, K., Engelkamp, D., Rassoulzadegan, M., Ross, A., Cuzin, F., van Heyningen, V., and Hastie, N.D. (1995). Subnuclear localization of *WT1* in splicing or transcription factor domains is regulated by alternative splicing. *Cell* 81, 391–401.

Lee, S.B., Huang, K., Palmer, R., Truong, V.B., Herzlinger, D., Kolquist, K.A., Wong, J., Paulding, C., Yoon, S.K., Gerald, W. (1999). The Wilms tumor suppressor *WT1* encodes a transcriptional activator of amphiregulin. *Cell* 98, 663–673.

Menke, A.L., van der Eb, A.J., and Jochemsen, A.G. (1998). The Wilms' tumor 1 gene: oncogene or tumor suppressor gene? *Int. Rev. Cytol.* 181, 151–212.

Miles, C., Elgar, G., Coles, E., Kleinjan, D.J., van Heyningen, V., and Hastie, N. (1998). Complete sequencing of the Fugu *WAGR* region

from WT1 to PAX6: dramatic compaction and conservation of synteny with human chromosome 11p13. *Proc. Natl. Acad. Sci. USA* 95, 13068–13072.

Moore, A.W., McInnes, L., Kreidberg, J., Hastie, N.D., and Schedl, A. (1999). YAC complementation shows a requirement for Wt1 in the development of epicardium, adrenal gland and throughout nephrogenesis. *Development* 126, 1845–1857.

Morais da Silva, S., Hacker, A., Harley, V., Goodfellow, P., Swain, A., and Lovell Badge, R. (1996). Sox9 expression during gonadal development implies a conserved role for the gene in testis differentiation in mammals and birds. *Nat. Genet.* 14, 62–68.

Nachtigal, M.W., Hirokawa, Y., Enyeart-VanHouten, D.L., Flanagan, J.N., Hammer, G.D., and Ingraham, H.A. (1998). Wilms' tumor 1 and Dax-1 modulate the orphan nuclear receptor SF-1 in sex-specific gene expression. *Cell* 93, 445–454.

Nagamine, C.M., Morohashi, K., Carlisle, C., and Chang, D.K. (1999). Sex reversal caused by *Mus musculus domesticus* Y chromosomes linked to variant expression of the testis-determining gene Sry. *Dev. Biol.* 216, 182–194.

Patek, C.E., Little, M.H., Fleming, S., Miles, C., Charlieu, J.P., Clarke, A.R., Miyagawa, K., Christie, S., Doig, J., Harrison, D.J. (1999). A zinc finger truncation of murine WT1 results in the characteristic urogenital abnormalities of Denys-Drash syndrome. *Proc. Natl. Acad. Sci. USA* 96, 2931–2936.

Putaal, H., Sainio, K., Sariola, H., and Tryggvason, K. (2000). Primary structure of mouse and rat nephrin cDNA and structure and expression of the mouse gene. *J. Am. Soc. Nephrol.* 11, 991–1001.

Shih, N.Y., Li, J., Karpitskii, V., Nguyen, A., Dustin, M.L., Kanagawa, O., Miner, J.H., and Shaw, A.S. (1999). Congenital nephrotic syndrome in mice lacking CD2-associated protein. *Science* 286, 312–315.

Shimamura, R., Fraizer, G.C., Trapman, J., Lau, Y.C., and Saunders, G.F. (1997). The Wilms' tumor gene WT1 can regulate genes involved in sex determination and differentiation: SRY, Mullerian-inhibiting substance, and the androgen receptor. *Clin. Cancer Res.* 3, 2571–2580.

Swain, A., Zanaria, E., Hacker, A., Lovell Badge, R., and Camerino, G. (1996). Mouse Dax1 expression is consistent with a role in sex determination as well as in adrenal and hypothalamus function. *Nat. Genet.* 12, 404–409.

Swain, A., Narvaez, V., Burgoyne, P., Camerino, G., and Lovell Badge, R. (1998). Dax1 antagonizes Sry action in mammalian sex determination. *Nature* 391, 761–767.

Toyooka, Y., Tanaka, S.S., Hirota, O., Tanaka, S., Takagi, N., Yamanouchi, K., Tojo, H., and Tachi, C. (1998). Wilms' tumor suppressor gene (WT1) as a target gene of SRY function in a mouse ES cell line transfected with SRY. *Int. J. Dev. Biol.* 42, 1143–1151.

Wagner, T., Wirth, J., Meyer, J., Zabel, B., Held, M., Zimmer, J., Pasantes, J., Bricarelli, F.D., Keutel, J., Hustert, E. (1994). Autosomal sex reversal and campomelic dysplasia are caused by mutations in and around the SRY-related gene SOX9. *Cell* 79, 1111–1120.

Wilkinson, D.G. (1992). Whole mount *in situ* hybridization of vertebrate embryos. In *In Situ Hybridization*, D.G. Wilkinson, ed. (Oxford: Oxford University Press), pp. 75–83.

Willnow, T.E., and Herz, J. (1994). Homologous recombination for gene replacement in mouse cell lines. *Methods Cell Biol.* 43A, 305–334.